


# Compact, charged boson stars and shells in the $\mathbb{C}P^N$ gravitating nonlinear sigma model

Nobuyuki Sawado<sup>\*</sup> and Shota Yanai<sup>†</sup>

*Department of Physics, Tokyo University of Science, Noda, Chiba 278-8510, Japan*

 (Received 10 June 2020; accepted 27 July 2020; published 6 August 2020)

We study  $U(1)$  gauged gravitating compact  $Q$ -ball,  $Q$ -shell solutions in a nonlinear sigma model with the target space  $\mathbb{C}P^N$ . The models with odd integer  $N$  and a special potential can be parameterized by  $N$ th complex scalar fields and they support compact solutions. By implementing the  $U(1)$  gauge field in the model, the behavior of the solutions becomes complicated than the global model. Especially, they have branches, i.e., two independent solutions with the same shooting parameter. The energy of the solutions in the first branch behaves as  $E \sim Q^{5/6}$  for small  $Q$ , where  $Q$  stands for the  $U(1)$  Noether charge. For the large  $Q$ , it gradually deviates from the scaling  $E \sim Q^{5/6}$  and, for the  $Q$ -shells it is  $E \sim Q^{7/6}$ , which forms the second branch. A coupling with gravity allows for harboring of the Schwarzschild black holes for the  $Q$ -shell solutions, forming the charged boson shells. The space-time then consists of a charged black hole in the interior of the shell, surrounded by a  $Q$ -shell, and the outside becomes a Reissner-Nordström space-time. These solutions inherit the scaling behavior of the flat space-time.

DOI: [10.1103/PhysRevD.102.045007](https://doi.org/10.1103/PhysRevD.102.045007)

## I. INTRODUCTION

A complex scalar field theory with some self-interactions has stationary soliton solutions called  $Q$ -balls [1–4].  $Q$ -balls have attracted much attention in the studies of evolution of the early Universe [5,6]. In supersymmetric extensions of the standard model,  $Q$ -balls appear as the scalar superpartners of baryons or leptons forming coherent states with baryon or lepton number. They may survive as a major ingredient of dark matter [7–9]. The  $U(1)$  invariance of the scalar field leads to the conserved charge  $Q$  which, if the theory is coupled with the electromagnetism it identifies as the electric charge of the constituents.

Our analysis is based on the model defined in  $3+1$  dimensions and it has the Lagrangian density

$$\mathcal{L} = -\frac{M^2}{2} \text{Tr}(X^{-1} \partial_\mu X)^2 - \mu^2 V(X), \quad (1)$$

where the “V-shaped” potential

$$V(X) = \frac{1}{2} [\text{Tr}(I - X)]^{1/2} \quad (2)$$

is employed for constructing the compact solutions. The behavior of fields at the outer border of compacton implies  $X \rightarrow I$ . The coupling constants  $M$ ,  $\mu$  have dimensions of  $(\text{length})^{-1}$  and  $(\text{length})^{-2}$ , respectively. The principal variable  $X$  successfully parametrizes the coset space  $SU(N+1)/U(N) \sim \mathbb{C}P^N$ . The principal variable parametrized by complex fields  $u_i$  takes the form

$$X(g) = \begin{pmatrix} I_{N \times N} & 0 \\ 0 & -1 \end{pmatrix} + \frac{2}{\vartheta^2} \begin{pmatrix} -u \otimes u^\dagger & iu \\ iu^\dagger & 1 \end{pmatrix}, \quad (3)$$

where  $\vartheta := \sqrt{1 + u^\dagger \cdot u}$ . Thus, the  $\mathbb{C}P^N$  Lagrangian of the model (6) takes the form

$$\mathcal{L}_{\mathbb{C}P^N} = -M^2 g^{\mu\nu} \tilde{\tau}_{\nu\mu} - \mu^2 V, \quad (4)$$

where

$$\tilde{\tau}_{\nu\mu} = -\frac{4}{\vartheta^4} \partial_\mu u^\dagger \cdot \Delta^2 \cdot \partial_\nu u, \quad \Delta_{ij}^2 := \vartheta^2 \delta_{ij} - u_i u_j^*. \quad (5)$$

The model possesses the compactons [10] and also the compact boson stars [11]. Compactons are field configurations that exist on finite size supports. Outside this support, the field is identically zero. For example, the signum-Gordon model; i.e., the scalar field model with standard kinetic terms and V-shaped potential gives rise to such solutions [12,13]. Interestingly, when the scalar field is coupled with electromagnetism, the structure changes drastically.

<sup>\*</sup>sawadoph@rs.tus.ac.jp  
<sup>†</sup>phyana0513@gmail.com

*Published by the American Physical Society under the terms of the Creative Commons Attribution 4.0 International license. Further distribution of this work must maintain attribution to the author(s) and the published article's title, journal citation, and DOI. Funded by SCOAP<sup>3</sup>.*

Maxwell gauged solitons of nonlinear sigma model have been studied in many years. The gauged  $O(3)$  model [14], the baby-skyrmions [15,16], and the magnetic skyrmions [17],  $\mathbb{C}P^1$  model [18] are well-known examples. For  $\mathbb{C}P^N$ ,  $N > 1$ , there is a work for a  $\mathbb{C}P^2$  of Maxwell gauged model [19].

$Q$ -balls resulting from local  $U(1)$  symmetry are studied in the literature [20–28]. Such  $Q$ -balls may be unstable for large values of their charge because of the repulsion mediated by the gauge force and the fermions or the scalar fields with opposite charge may reduce such repulsions [21].

In the case of the compactons, when the scalar field is coupled with electromagnetism, then the inner radius emerges, i.e., the scalar field vanishes also in the central region  $r < R_{\text{in}}$ . Thus, the matter field exists in the region  $R_{\text{in}} \leq r \leq R_{\text{out}}$ . Such configurations of fields are called  $Q$ -shells. Such shell solutions have no restrictions on upper bound for  $|Q|$ . The authors claim that the energy of compact  $Q$ -balls scales as  $\sim Q^{5/6}$  and of  $Q$ -shells for large  $Q$  as  $\sim Q^{7/6}$ . It clearly indicates that the  $Q$ -balls are stable against the decay while the  $Q$ -shells may be unstable.

Boson stars are the gravitating objects of such  $Q$ -balls. There are a large number of articles concerning the boson stars [5,29–33]. The compact boson stars and shells are extensively studied in [11,31,32,34] for the global models and in [35–37] for the  $U(1)$  gauged model. For the boson shell configurations, one possibility is the case that the gravitating boson shells surround a flat Minkowski-like interior region  $r < R_{\text{in}}$  while the exterior region  $r > R_{\text{out}}$  is the exterior of a Reissner-Nordström solution. Another and even more interesting possibility is the existence of the charged black hole in the interior region. The gravitating boson shells can harbor a black hole. Since the black hole is surrounded by a shell of scalar fields, such fields outside of the event horizon may be interpreted as a scalar hair. Such possibility has been considered as contradiction of the no-hair conjecture [31,32]. The higher dimensional generalizations have been considered in [38,39].

The excited boson stars are very important not only of the theoretical interest and also for astrophysical observations [40–44]. The multistate boson stars which are a superposition of ground and excited states boson star solutions are considered for obtaining realistic rotation curves of spiral galaxies [41]. The authors of [43,44] proposed boson star solutions for a collection of an arbitrary odd number  $N$  of complex scalar fields with an internal symmetry  $U(N)$ . They are new excited solutions with angular momentum  $\ell$  so is dubbed as  $\ell$ -boson stars. Our  $\mathbb{C}P^N$  boson stars share many common features with them.

In this paper, we explore the  $U(1)$  gauged the gravitating boson shells. Properties of the harbor type solutions are also discussed. Especially we examine detailed energy scaling property about the  $\sim Q^{5/6}$  behavior for the gravitating, or the harbor type solutions.

The paper is organized as follows. In Sec. II, we shall describe the model, coupled to the gravitation. Ansatz for the parametrization of the  $\mathbb{C}P^N$  field is given in this section. Section III is analysis of in the flat space-time, i.e.,  $Q$ -balls and  $Q$ -shells. We give the gravitation solutions in Sec. IV. Scaling relation between the energy and the charge in the boson stars and shells is discussed in Sec. V. Conclusions and remarks are presented in the last section.

## II. THE MODEL

### A. The action, the equations of motion

We start with the action of self-gravitating complex fields  $u_i$  coupled to Einstein gravity,

$$S = \int d^4x \sqrt{-g} \left[ \frac{R}{16\pi G} - \frac{1}{4} g^{\mu\lambda} g^{\nu\sigma} F_{\mu\nu} F_{\lambda\sigma} - M^2 g^{\mu\nu} \tau_{\nu\mu} - \mu^2 V \right], \quad (6)$$

$$\tau_{\nu\mu} = -\frac{4}{g^4} D_\mu u^\dagger \cdot \Delta^2 \cdot D_\nu u, \quad \Delta_{ij}^2 := \vartheta^2 \delta_{ij} - u_i u_j^*, \quad (7)$$

where  $G$  is Newton's gravitational constant.  $F_{\mu\nu}$  is the standard electromagnetic field tensor and the complex fields  $u_i$  also are minimally coupled to the Abelian gauge fields  $A_\mu$  through  $D_\mu = \partial_\mu - ieA_\mu$ .

The variation of the action with respect to the metric leads to Einstein's equations,

$$G_{\mu\nu} = 8\pi G T_{\mu\nu}, \quad \text{where } G_{\mu\nu} \equiv R_{\mu\nu} - \frac{1}{2} g_{\mu\nu} R, \quad (8)$$

where the stress-energy tensor reads

$$T_{\mu\nu} = g_{\mu\nu} \left( M^2 g^{\lambda\sigma} \tau_{\sigma\lambda} + \frac{1}{4} g^{\lambda\sigma} g^{\eta\delta} F_{\lambda\eta} F_{\sigma\delta} + \mu^2 V \right) - 2M^2 \tau_{\nu\mu} - g^{\lambda\sigma} F_{\mu\lambda} F_{\nu\sigma}. \quad (9)$$

The field equations of the complex fields are obtained by variation of the Lagrangian with respect to  $u_i^*$ ,

$$\frac{1}{\sqrt{-g}} D_\mu (\sqrt{-g} D^\mu u_i) - \frac{2}{\vartheta^2} (u^\dagger \cdot D^\mu u) D_\mu u_i + \frac{\mu^2}{4M^2} \vartheta^2 \sum_{k=1}^N \left[ (\delta_{ik} + u_i u_k^*) \frac{\partial V}{\partial u_k^*} \right] = 0. \quad (10)$$

The Maxwell's equations read

$$\frac{1}{\sqrt{-g}} \partial_\nu (\sqrt{-g} F^{\nu\mu}) = \frac{4ie}{g^4} M^2 (u^\dagger \cdot D^\mu u - D^\mu u^\dagger \cdot u). \quad (11)$$

It is convenient to introduce the dimensionless coordinates

$$x_\mu \rightarrow \frac{\mu}{M} x_\mu \quad (12)$$

and also  $A_\mu \rightarrow \mu/MA_\mu$ . We also restrict  $N$  to be odd, i.e.,  $N := 2n + 1$ . For solutions with vanishing magnetic field, the ansatz has the form

$$u_m(t, r, \theta, \varphi) = \sqrt{\frac{4\pi}{2n+1}} f(r) Y_{nm}(\theta, \varphi) e^{i\omega t}, \quad (13)$$

$$A_\mu(t, r, \theta, \varphi) dx^\mu = A_t(r) dt \quad (14)$$

that allows for reduction of the partial differential equations to the system of radial ordinary differential equations.  $Y_{nm}$ ,  $-n \leq m \leq n$  are the standard spherical harmonics and  $f(r)$  is the profile function. Each  $2n + 1$  field  $u = (u_m) = (u_{-n}, u_{-n+1}, \dots, u_{n-1}, u_n)$  is associated with one of  $2n + 1$  spherical harmonics for given  $n$ . The relation  $\sum_{m=-n}^n Y_{nm}^*(\theta, \varphi) Y_{nm}(\theta, \varphi) = \frac{2n+1}{4\pi}$  is very useful for obtaining an explicit form of many inner products. We introduce a new gauge field concerning the gauge field for convenience,

$$b(r) := \omega - eA_t(r). \quad (15)$$

Using the ansatz, we find the dimensionless Lagrangian of the  $\mathbb{C}P^N$  model in the form

$$\begin{aligned} \tilde{\mathcal{L}}_{\mathbb{C}P^N} &= -\frac{\kappa}{4} g^{\mu\lambda} g^{\nu\sigma} F_{\mu\nu} F_{\lambda\sigma} - g^{\mu\nu} \tau_{\nu\mu} - V \\ &= \frac{\kappa b^2}{2A^2 e^2} + \frac{4b^2 f^2}{A^2 C(1+f^2)^2} - \frac{4Cf^2}{(1+f^2)^2} \\ &\quad - \frac{4n(n+1)f^2}{r^2(1+f^2)} - V, \end{aligned} \quad (16)$$

where we have introduced a dimensionless constant  $\kappa := \mu^2/M^4$  for convenience.

There is a symmetry  $b \rightarrow -b$ , i.e.,  $\omega \rightarrow -\omega$ ,  $eA_t \rightarrow -eA_t$  in (16), so one can simply assume that  $\omega \geq 0$  [20]. In this paper, we shall not adopt the above symmetry and examine the case with both signs of  $\omega$ . We shall see that our obtained solutions always satisfy  $b > 0$ , and the Noether charge is positive definite.

For the ansatz (13)–(15), a suitable form of line element is the standard spherically symmetric Schwarzschild-like coordinates defined by

$$\begin{aligned} ds^2 &= g_{\mu\nu} dx^\mu dx^\nu \\ &= A^2(r) C(r) dt^2 - \frac{1}{C(r)} dr^2 - r^2(d\theta^2 + \sin^2\theta d\varphi^2). \end{aligned} \quad (17)$$

Substituting (17) and (13)–(15) into the Einstein field equations (8), we get their components,

$$\begin{aligned} (tt): \frac{[r(1-C)]'}{r^2} &= \alpha \left[ \frac{4b^2 f^2}{A^2 C(1+f^2)^2} + \frac{4Cf^2}{(1+f^2)^2} \right. \\ &\quad \left. + \frac{4n(n+1)f^2}{r^2(1+f^2)} + \frac{\kappa b^2}{2e^2 A^2} + \frac{f}{\sqrt{1+f^2}} \right], \end{aligned} \quad (18)$$

$$\begin{aligned} (rr): \frac{2rCA' - A[r(1-C)]'}{r^2 A} &= \alpha \left[ \frac{4b^2 f^2}{A^2 C(1+f^2)^2} \right. \\ &\quad \left. + \frac{4Cf^2}{(1+f^2)^2} - \frac{4n(n+1)f^2}{r^2(1+f^2)} - \frac{\kappa b^2}{2A^2 e^2} - \frac{f}{\sqrt{1+f^2}} \right], \end{aligned} \quad (19)$$

$$\begin{aligned} (\theta\theta): \frac{3rA'C' + 2C(A' + rA'') + A(2C' + rC'')}{2rA} \\ = \alpha \left[ \frac{4b^2 f^2}{A^2 C(1+f^2)^2} - \frac{4Cf^2}{(1+f^2)^2} + \frac{\kappa b^2}{2A^2 e^2} - \frac{f}{\sqrt{1+f^2}} \right], \end{aligned} \quad (20)$$

where  $\alpha$  is a dimensionless coupling constant concerning to the gravity

$$\alpha := 8\pi G\mu^2. \quad (21)$$

From (18) and (19), one can construct the equations of motion of  $A(r)$ ,  $C(r)$ ,

$$A' = 4\alpha r \left[ \frac{b^2 f^2}{A^2 C^2(1+f^2)^2} + \frac{f^2}{(1+f^2)^2} \right], \quad (22)$$

$$\begin{aligned} C' &= \frac{1-C}{r} \\ &\quad - \alpha r \left[ \frac{4b^2 f^2}{A^2 C(1+f^2)^2} + \frac{4Cf^2}{(1+f^2)^2} + \frac{4n(n+1)f^2}{(1+f^2)r^2} \right. \\ &\quad \left. + \frac{\kappa b^2}{2A^2 e^2} + \frac{f}{\sqrt{1+f^2}} \right]. \end{aligned} \quad (23)$$

Plugging the ansatz (13)–(15) into the matter field equation (10) and the Maxwell's equations (11), we have

$$\begin{aligned} C f'' + C' f' + \frac{A' C f'}{A} + \frac{2C}{r} f' - \frac{n(n+1)f}{r^2} \\ + \frac{(1-f^2)b^2 f}{A^2 C(1+f^2)} - \frac{2C f f^2}{(1+f^2)} - \frac{1}{8} \sqrt{1+f^2} = 0, \end{aligned} \quad (24)$$

$$\kappa b'' + \frac{2r'A - A'r}{Ar} \kappa b' - \frac{8e^2}{C} \frac{b f^2}{(1+f^2)^2} = 0. \quad (25)$$

Thus, we solve a four coupled equations (22)–(25) varying the parameters  $\alpha$  with fixed  $\kappa$ ,  $e$  (in this paper, we simply set  $\kappa = e = 1$ ).

The dimensionless Hamiltonian of the model is easily obtained,

$$\begin{aligned} \mathcal{H}_{\mathbb{C}P^N} &= \frac{\partial \tilde{\mathcal{L}}_{\mathbb{C}P^N}}{\partial(\partial_0 u_i^*)} \partial_0 u_i^* + \frac{\partial \tilde{\mathcal{L}}_{\mathbb{C}P^N}}{\partial(\partial_0 u_i)} \partial_0 u_i - \tilde{\mathcal{L}}_{\mathbb{C}P^N} \\ &= \frac{8\omega b f^2}{A^2 C(1+f^2)^2} - \frac{\kappa b'^2}{2A^2 e^2} - \frac{4b^2 f^2}{A^2 C(1+f^2)^2} \\ &\quad + \frac{4Cf'^2}{(1+f^2)^2} + \frac{4n(n+1)f^2}{r^2(1+f^2)} + V. \end{aligned} \quad (26)$$

The total energy is thus given by

$$\begin{aligned} E &= 4\pi \int r^2 dr \left[ \frac{\kappa b'^2}{2Ae^2} + \frac{4b^2 f^2}{AC(1+f^2)^2} \right. \\ &\quad \left. + \frac{4ACf'^2}{(1+f^2)^2} + \frac{4An(n+1)f^2}{r^2(1+f^2)} + AV \right]. \end{aligned} \quad (27)$$

### B. The Noether charge

The symmetry of the matter field is  $SU(N) \otimes U(1)$ . Since it contains the  $U(1)^N$  symmetry subgroup, then following Ref. [19], we consider a covariant derivative for the  $\mathbb{C}P^N$  field,

$$D_\mu u_i = \partial_\mu u_i - ieA_\mu Q_{ij} u_j, \quad (28)$$

where  $Q_{ij}$  is some real diagonal matrix  $Q_{ij} = \text{diag}(q_1, \dots, q_N)$ . The action (6) with the covariant derivative is invariant under following local  $U(1)^N$  symmetry:

$$\begin{aligned} A_\mu(x) &\rightarrow A_\mu(x) + e^{-1} \partial_\mu \Lambda(x) \\ u_i &\rightarrow \exp[iq_i \Lambda(x)] u_i, \quad i = 1, \dots, N. \end{aligned} \quad (29)$$

The following Noether current is associated with the invariance of the action (6) under transformations (29):

$$J_\mu^{(i)} = -\frac{4M^2 i}{g^4} \sum_{j=1}^N [u_i^* \Delta_{ij}^2 D_\mu u_j - D_\mu u_j^* \Delta_{ji}^2 u_i]. \quad (30)$$

Using the ansatz (13), (14), we find the following form of the Noether currents:

$$J_t^{(m)} = \frac{(n-m)!}{(n+m)!} \frac{8bf^2}{(1+f^2)^2} (P_n^m(\cos\theta))^2, \quad (31)$$

$$J_\varphi^{(m)} = \frac{(n-m)!}{(n+m)!} \frac{8mf^2}{(1+f^2)^2} (P_n^m(\cos\theta))^2, \quad (32)$$

and  $J_r^{(m)} = J_\theta^{(m)} = 0$  for  $m = -n, -n+1, \dots, n-1, n$ . The conservation of currents is explicit after writing the continuity equation in the form

$$\frac{1}{\sqrt{-g}} \partial_\mu (\sqrt{-g} g^{\mu\nu} J_\nu^{(m)}) = \frac{1}{A^2 C} \partial_t J_t^{(m)} + \frac{1}{r^2 \sin^2 \theta} \partial_\varphi J_\varphi^{(m)} = 0. \quad (33)$$

Therefore, the corresponding Noether charge is

$$\begin{aligned} Q^{(m)} &= \frac{1}{2} \int_{\mathbb{R}^3} d^3 x \sqrt{-g} \frac{1}{A^2 C} J_t^{(m)}(x) \\ &= \frac{16\pi}{2n+1} \int r^2 dr \frac{bf^2}{AC(1+f^2)^2}. \end{aligned} \quad (34)$$

Owing to our ansatz, the charge does not depend on index  $m$ , which means the symmetry of the solutions is reduced to the  $U(1)$ . However, we shall keep the index for completeness.

The spatial components of the Noether currents do not contribute to the charges; however, they can be used to introduce some auxiliary integrals [11],

$$\begin{aligned} q^{(m)} &= \frac{3}{2} \int d^3 x \sqrt{-g} \frac{J_\varphi^{(m)}(x)}{r^2} \\ &= \frac{48\pi m}{2n+1} \int_0^\infty dr \frac{Af^2}{1+f^2}. \end{aligned} \quad (35)$$

As in the case of the gauged  $Q$ -balls [20], and also in the compactons [13], the total energy of our gauged model can be expressed using these Noether charges. For the  $Q$ -shells, the function  $f(r)$  vanishes for  $r < R_{\text{in}}$  and  $r > R_{\text{out}}$ , so the Noether charge  $Q^{(m)}$  is

$$Q^{(m)} = \frac{16\pi}{2n+1} \int_{R_{\text{in}}}^{R_{\text{out}}} r^2 dr \frac{bf^2}{AC(1+f^2)^2}. \quad (36)$$

Equation (25) is written in the compact form

$$\kappa \left( r^2 \frac{b'}{A} \right)' = \frac{8e^2 r^2}{AC} \frac{bf^2}{(1+f^2)^2}. \quad (37)$$

A single integration gives the expression

$$b'(r) = \frac{1}{r^2} \frac{8e^2 A(r)}{\kappa} \int_0^r r'^2 dr' \frac{b(r') f(r')^2}{A(r') C(r') (1+f(r')^2)^2}, \quad (38)$$

which implies that the function  $b(r)$  is a monotonically increasing function. Therefore, for sufficiently large  $r (> R_{\text{out}})$ ,  $b'(r) = \bar{Q}/r^2$  ( $\bar{Q} > 0$ ), where

$$\bar{Q} \equiv \frac{8e^2 A}{\kappa} \int_{R_{\text{in}}}^{R_{\text{out}}} r^2 dr \frac{bf^2}{AC(1+f^2)^2} = \frac{e^2 A(2n+1)}{2\pi\kappa} Q^{(m)}, \quad (39)$$

where we have used the boundary condition  $A(\infty) \equiv 1$ . Thus, we obtain  $b(r)$  for large  $r$ ,

$$b(r) = \omega - \frac{\bar{Q}}{r}. \quad (40)$$

$A_l$  behaves as  $A_l = \bar{Q}/er$  for large  $r$ , and therefore it can be interpreted as the Coulomb potential of the spherically symmetric charge distribution in the compact region. The second term of the right-hand side of (27) can be evaluated by the partial integration

$$\begin{aligned} \frac{1}{2} \int r^2 dr \frac{\kappa b'^2}{Ae^2} &= \frac{\kappa}{2} \left[ r^2 \frac{b'b}{Ae^2} \right]_0^\infty - \frac{\kappa}{2} \int dr b \left( r^2 \frac{b'}{Ae^2} \right)' \\ &= \frac{\kappa}{2} \left( r^2 \frac{b'b}{Ae^2} \right) \Big|_{r \rightarrow \infty} - \frac{1}{2} \int dr \frac{8r^2}{AC} \frac{b^2 f^2}{(1+f^2)^2}, \end{aligned} \quad (41)$$

where we have used (37). The first term of the right-hand side can be evaluated with (39) and with the asymptotic behavior of  $b$  (40),

$$r^2 \frac{b'b}{Ae^2} \Big|_{r \rightarrow \infty} = r^2 \frac{1}{A2e^2} \omega \left( \frac{\bar{Q}}{r^2} \right) = \omega \frac{(2n+1)}{2\pi\kappa} Q^{(m)}. \quad (42)$$

As a result, we obtain the total energy for large  $r$  of the form

$$\begin{aligned} E &= \sum_{m=-n}^n (\omega Q^{(m)} + m q^{(m)}) \\ &+ 4\pi \int r^2 dr A \left( \frac{4Cf'^2}{(1+f^2)^2} + V \right). \end{aligned} \quad (43)$$

This form is similar of the nongauged case [11].

For the full understanding of the gauged  $Q$ -ball boson stars, we need to know  $E$  as function of  $Q$ . Only limited cases such like a thin-wall approximation of the model in a flat space-time might be possible, but for the gravitating case, we have to rely on the numerical analysis.

### C. The boundary behavior of solutions

We examine behavior of solutions at the boundary, which means that we mainly look at the origin  $r = 0$  and the border(s) of the compacton. First, we consider expansion at the origin and so the solution is represented by series

$$\begin{aligned} f(r) &= \sum_{k=0}^{\infty} f_k r^k, & b(r) &= \sum_{k=0}^{\infty} b_k r^k, \\ A(r) &= \sum_{k=0}^{\infty} A_k r^k, & C(r) &= \sum_{k=-2}^{\infty} C_k r^k. \end{aligned} \quad (44)$$

After substituting these expressions into Eqs. (22)–(25), one requires vanishing of equations in all orders of expansion. It allows us to determinate the coefficients of

expansion. The form is given for each value of parameter  $n$ . For  $n = 0$ , it reads

$$\begin{aligned} f(r) &= f_0 + \frac{1}{48} \left( \sqrt{1+f_0^2} - \frac{8f_0(1-f_0^2)b_0^2}{A_0^2(1+f_0^2)} \right) r^2 + O(r^4), \\ b(r) &= b_0 + \frac{4e^2 b_0^2 f_0^2}{3(1+f_0^2)^2} r^2 + O(r^4), \end{aligned} \quad (45)$$

$$\begin{aligned} A(r) &= A_0 + \frac{2\alpha f_0^2 b_0^2}{A_0(1+f_0^2)^2} r^2 + O(r^4), \\ C(r) &= 1 - \frac{\alpha}{3} \left( \frac{f_0}{\sqrt{1+f_0^2}} + \frac{4f_0^2 b_0^2}{A_0^2(1+f_0^2)^2} \right) r^2 + O(r^4), \end{aligned} \quad (46)$$

where  $f_0$ ,  $b_0$ , and  $A_0$  are free parameters. For  $n = 1$ , we obtain

$$\begin{aligned} f(r) &= f_1 r + \frac{1}{32} r^2 + \frac{1}{10} \left( 2f_1^3(1+6\alpha) - \frac{f_1 b_0^2}{A_0^2} \right) r^3 \\ &+ O(r^4), \\ b(r) &= b_0 + \frac{2}{5} e^2 f_1^2 b_0 r^4 + O(r^5), \end{aligned} \quad (47)$$

$$\begin{aligned} A(r) &= A_0 + \alpha A_0 f_1^2 r^2 + \frac{1}{6} \alpha A_0 f_1 r^3 + O(r^4), \\ C(r) &= 1 - 4\alpha f_1^2 r^2 - \frac{\alpha f_1}{2} r^3 + O(r^4), \end{aligned} \quad (48)$$

with free parameters  $f_1$ ,  $b_0$ , and  $A_0$ .

For  $n \geq 2$ , we have no nontrivial solutions at the vicinity of the origin  $r = 0$ , then the solution has to be identically zero. In order to get nontrivial solution, we consider a possibility that the solution does not vanish only inside the shell having radial support  $r \in (R_{\text{in}}, R_{\text{out}})$ . Solutions of this kind are called  $Q$ -shells. We study expansion at the sphere with an inner or an outer radius. Expansions at both borders of the compacton are very similar. We impose the following boundary conditions at the compacton radius  $r = R (\equiv R_{\text{in}}, R_{\text{out}})$ :

$$f(R) = 0, \quad f'(R) = 0, \quad A(R) = 1. \quad (49)$$

The functions  $f(r)$ ,  $b(r)$ ,  $A(r)$ , and  $C(r)$  are represented by series

$$\begin{aligned} f(r) &= \sum_{k=2}^{\infty} F_k (R-r)^k, & b(r) &= \sum_{k=0}^{\infty} B_k (R-r)^k, \\ A(r) &= \sum_{k=0}^{\infty} A_k (R-r)^k, & C(r) &= \sum_{k=-2}^{\infty} C_k (R-r)^k. \end{aligned} \quad (50)$$

First few terms have the form

$$\begin{aligned}
 f(r) &= \frac{R}{16C_0}(R-r)^2 + \frac{R}{24C_0^2}(R-r)^3 + O((R-r)^4), \\
 b(r) &= B_0 + B_1(R-r) - \frac{B_1}{R}(R-r)^2 + \frac{B_1}{3R^2}(R-r)^3 \\
 &\quad + O((R-r)^4), \\
 A(r) &= A_0 - \frac{\alpha R}{48C_0^2}(R-r)^3 + O((R-r)^4), \\
 C(r) &= C_0 + \frac{1-C_0}{R}(R-r) \\
 &\quad + \left\{ (C_0-1)\frac{1}{R_0^2} - \frac{5\alpha B_1^2}{4A_0^2 e^2} \right\} (R-r)^2 \\
 &\quad + O((R-r)^3). \tag{51}
 \end{aligned}$$

For electrically charged black hole solutions in the interior of the shell, we impose the boundary conditions for the functions  $b(r)$ ,  $C(r)$  at the inner radius  $r = R_{\text{in}}$ ,

$$\begin{aligned}
 C(R_{\text{in}}) &= 1 - \frac{2M_{\text{H}}}{R_{\text{in}}} + \frac{Q_{\text{H}}^2}{R_{\text{in}}^2}, \\
 b(R_{\text{in}}) &= b_0 - \frac{B_c}{R_{\text{in}}}, \quad b'(R_{\text{in}}) = \frac{B_c}{R_{\text{in}}^2}, \tag{52}
 \end{aligned}$$

where

$$M_{\text{H}} = \frac{1}{2} \left( r_{\text{H}} + \frac{Q_{\text{H}}^2}{r_{\text{H}}} \right), \quad B_c = \frac{Q_{\text{H}} A_0 e \sqrt{2}}{\sqrt{\alpha}}, \tag{53}$$

and  $Q_{\text{H}}$  is the horizon charge.

### III. THE SOLUTIONS IN THE FLAT SPACE-TIME

We begin with the numerical analysis of  $Q$ -balls and  $Q$ -shells in flat space-time. We solve the coupled differential Eqs. (24) and (25) by a shooting method. According to (46) and (48), the solutions with  $n = 0, 1$  are regular at the origin and then they are  $Q$ -ball type solutions. The solution of  $n = 0$  is plotted in Fig. 1. The profile functions  $f(r)$  are nonzero at the origin and monotonically approach

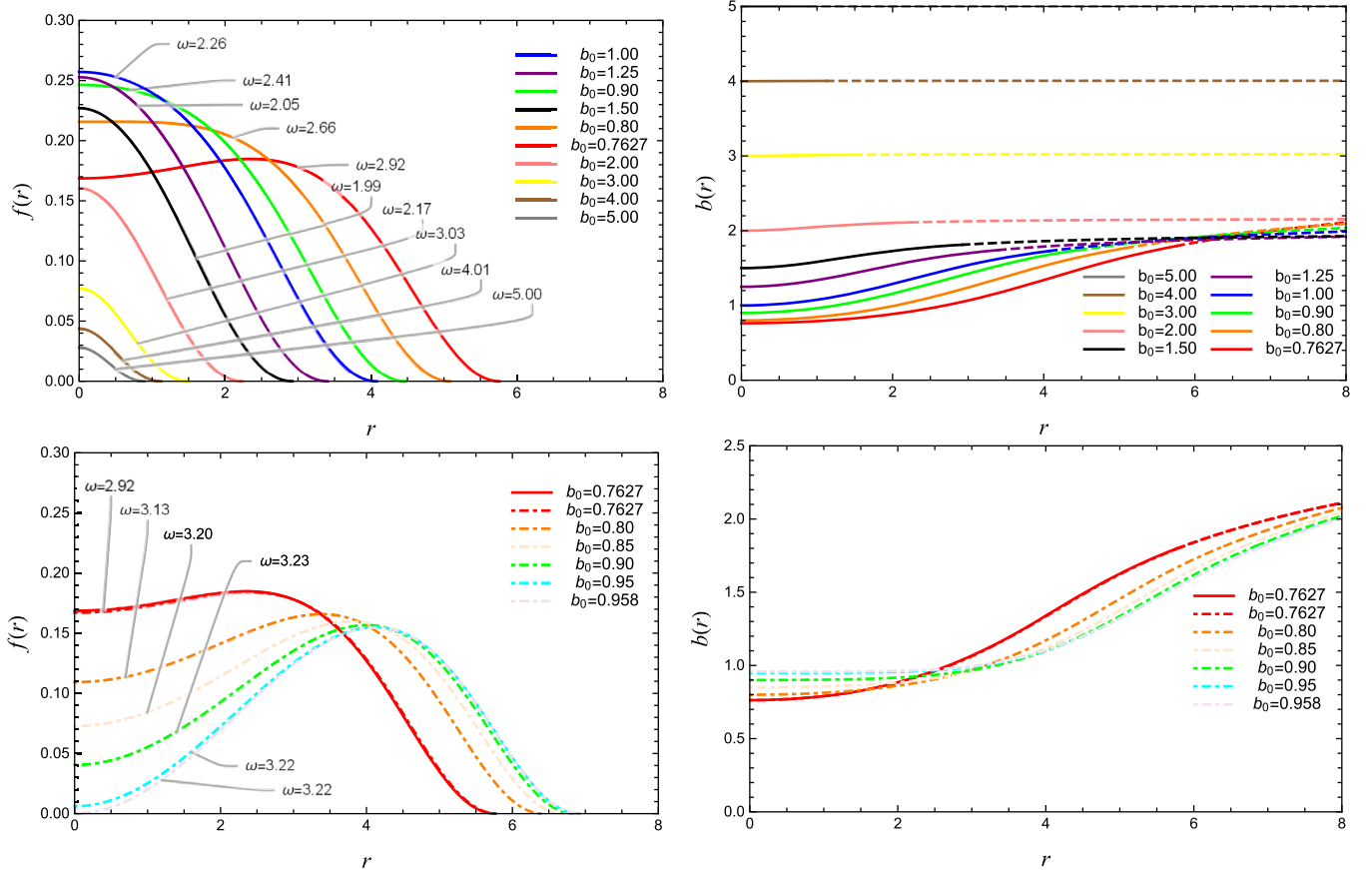


FIG. 1. The gauged  $Q$ -ball solution for the  $CP^1$  case. Top left: the matter profile function  $f(r)$  of the first branch. Top right: The gauge function  $b(r)$  of the first branch. Bottom left: The matter profile function  $f(r)$  of the second branch. Bottom right: the gauge function  $b(r)$  of the second branch. Solutions of the first branch are plotted with the bold line and those of the second branch are plotted with the dot-dashed line. Solutions of the vacuum equations are depicted with the dashed line. Distinct curves correspond with different values of the shooting parameter  $b_0$ .

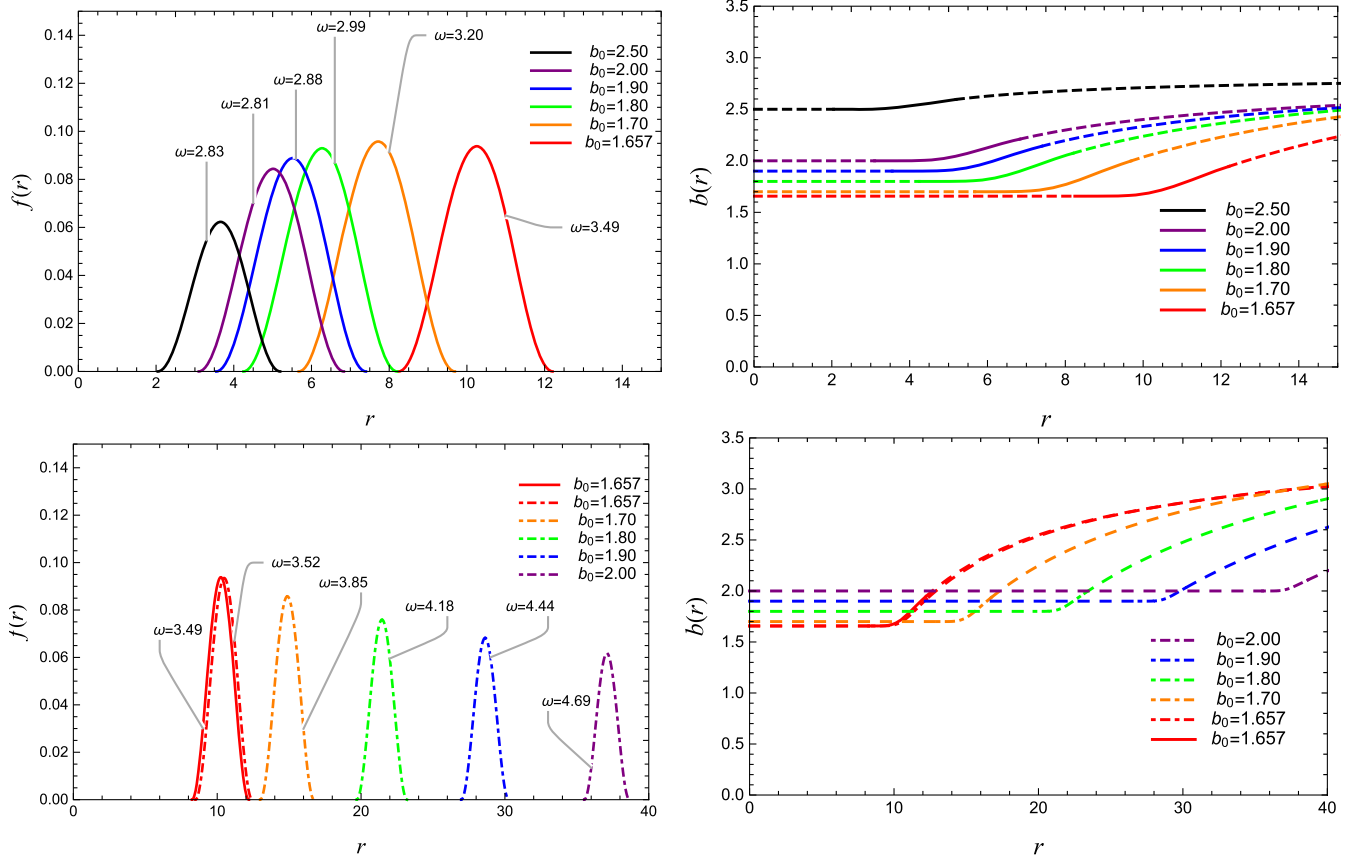


FIG. 2. The gauged  $Q$ -shell solution for the  $\mathbb{C}P^{11}$  case. Top left: the matter profile function  $f(r)$  of the first branch. Top right: the gauge function  $b(r)$  of the first branch. Bottom left: the matter profile function  $f(r)$  of the second branch. Bottom right: the gauge function  $b(r)$  of the second branch. Solutions of the first branch are plotted with the bold line and those of the second branch are plotted with the dot-dashed line. Solutions of the vacuum equations are depicted with the dashed line. Distinct curves correspond with different values of the shooting parameter  $b_0$ .

zero of the compaction radius, which is similar behavior with the nongauged solution discussed in [11]. We have two independent shooting parameters  $f_0$ ,  $b_0$ , and for the moment we fix  $b_0$  and varies  $f_0$  for finding solutions. The value of the  $\omega$  is depicted via the asymptotic behavior of the numerical solution of  $b(r)$ , which obeys (40). A notable feature of our solutions is that there are branches, i.e., two types of the solutions with equal values of shooting parameter, which exhibit a notable difference for varying  $\omega$ . In Fig. 1, we present the typical behavior. The first type of solutions (the bold lines) exhibit the lumplike shape, i.e., peaked at the origin. For smaller the shooting parameters  $b_0$ , the solutions  $f(r)$  grow. On the other hand, the second type of solutions (the dot-dashed lines) have a dip, i.e., the peaks are located outside, not at the origin. The bifurcation point is on  $b_0 = 0.7627$ , where the two solutions join. Interestingly, some of the solutions of the first type ( $b_0 = 0.7627$  and  $0.80$ ) look interpolating between the branches. The first and the second type solutions smoothly connect via these intermediate solutions.

As we posed in the previous section, the solutions are not regular at the origin for  $n \geq 2$ , which then leads to the

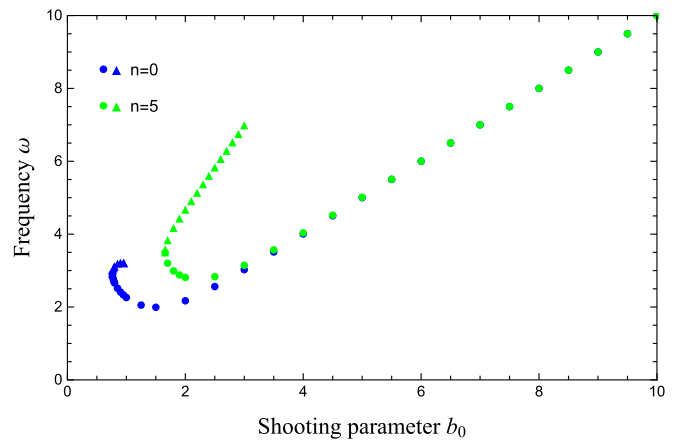


FIG. 3. A relation between shooting parameter  $b_0$  and frequency  $\omega$  for  $\mathbb{C}P^1$  (blue) and  $\mathbb{C}P^{11}$  (green). The dots correspond to solutions with different  $\omega$  of the first branch and the triangles to the second branch.

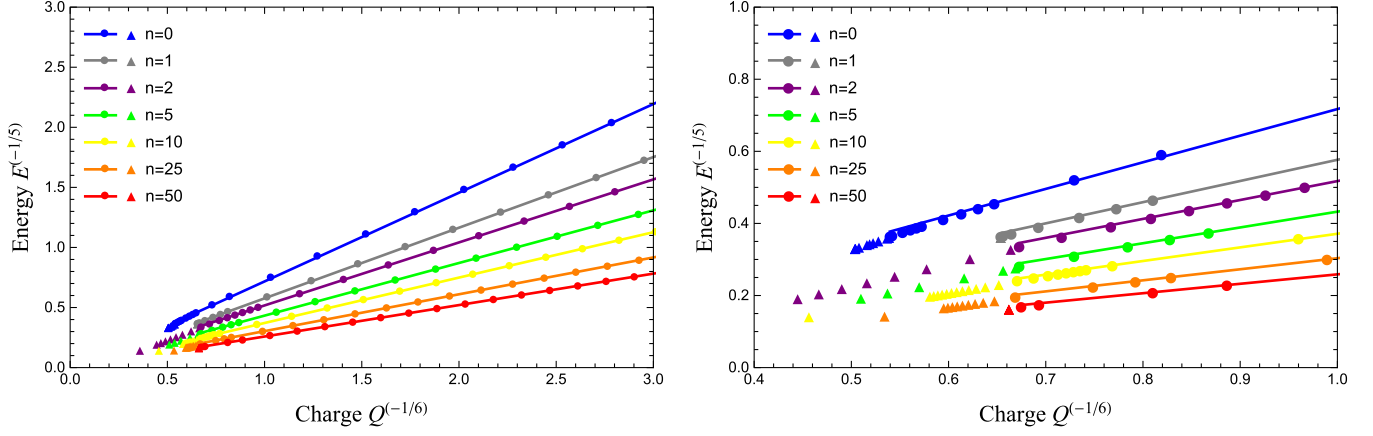


FIG. 4. Left: the relation between  $E^{-1/5}$  and  $Q^{-1/6}$  for several gauged solutions. Right: the same as the left one but the plot is enlarged in the region of high  $Q$ ,  $E$ . The dots correspond to solutions of the first branch. The triangles correspond to solutions of the second branch.

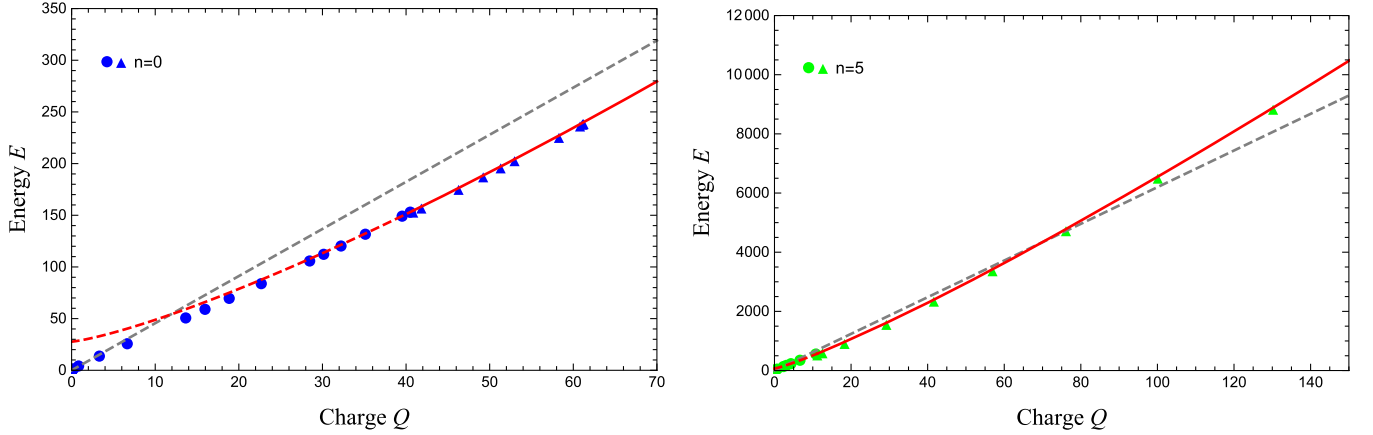


FIG. 5. The relation between  $E$  and  $Q$ . Left:  $\mathbb{C}P^1$ . Right:  $\mathbb{C}P^{11}$ . The gray dashed lines indicate  $E = \beta^{-5}Q$ , where  $\beta$  is the gradient of  $E^{-1/5} - Q^{-1/6}$  in Fig. 4. We numerically fit the data of the solutions in the second branch with  $E = \eta Q^\alpha + \xi$ . The resultant functions are shown as the red line. For  $\mathbb{C}P^1$ ,  $\eta = 1.12327$ ,  $\xi = 24.7417$ ,  $\alpha = 1.27389$ . For  $\mathbb{C}P^{11}$ ,  $\eta = 30.0064$ ,  $\xi = 68.5474$ ,  $\alpha = 1.16711 \sim 7/6$ .

$Q$ -shells, i.e., the matter field is localized in the radial segment  $r \in (R_{\text{in}}, R_{\text{out}})$  and the gauge field  $b(r)$  is of a constant at the interior region  $r < R_{\text{in}}$  and of the asymptotic solution (40) at the exterior  $r > R_{\text{out}}$ . Some typical solutions are shown in Fig. 2. Similar with the cases of the  $Q$ -balls, we obtain two types of the solutions which join at  $b_0 = 1.657$ . The peak of the solutions moves outside as  $\omega$  grows. Especially the second type of solutions rapidly expand as  $\omega$  increases. In Fig. 3, we plot the relation between the shooting parameter  $b_0$  and the corresponding frequency  $\omega$  for  $\mathbb{C}P^1$  and  $\mathbb{C}P^{11}$ .

For the stability of the  $Q$ -balls, we examine the energy-Noether charge scaling relation. In the studies for the global model, it was shown that the relation  $E \sim Q^{5/6}$  strictly holds for the solutions in flat space-time [10] and for several gravitating solutions [11]. Thus, it is natural to investigate the relation between  $E^{-1/5}$  and  $Q^{-1/6}$  in the present model. In Fig. 4, we plot the relation for  $n = 0, 1, 2,$

$5, 10, 25, 50$ . The dots indicate the solutions with different frequency  $\omega$ . In each  $n$ , most of the points lie on the straight line with certain good accuracy. However, the data deviate from the linearity especially for larger  $Q$  or  $E$  and indicate for large  $Q$  the energy scales different from  $\sim Q^{5/6}$ . Figure 5 is an analysis of the relation between  $Q$  and  $E$  for  $\mathbb{C}P^1$  and  $\mathbb{C}P^{11}$ , where the data are depicted from result of Fig. 4, which are compared to the dotted lines  $E = \beta^{-1/5}Q$ . The coefficient  $\beta$  is extracted from the slope in Fig. 4, i.e.,  $E^{-1/5} = \beta Q^{-1/6}$ . For the  $Q$ -ball, the energy is lower than the linear behavior. The  $Q$ -shell solutions have the energy enhanced than the linearity. We study a power law of the scaling with numerically fitting the data for the second type of solutions. For the  $Q$ -shell, it is  $1.176711 \sim 7/6$ . This scaling is in good agreement with the result of  $Q$ -shell in the signum-Gordon model [13]. The  $Q$ -ball solution has the power  $\sim 1.2739$ , higher than  $7/6$ , which is a consequence of the boundary behavior at the origin. For growing the



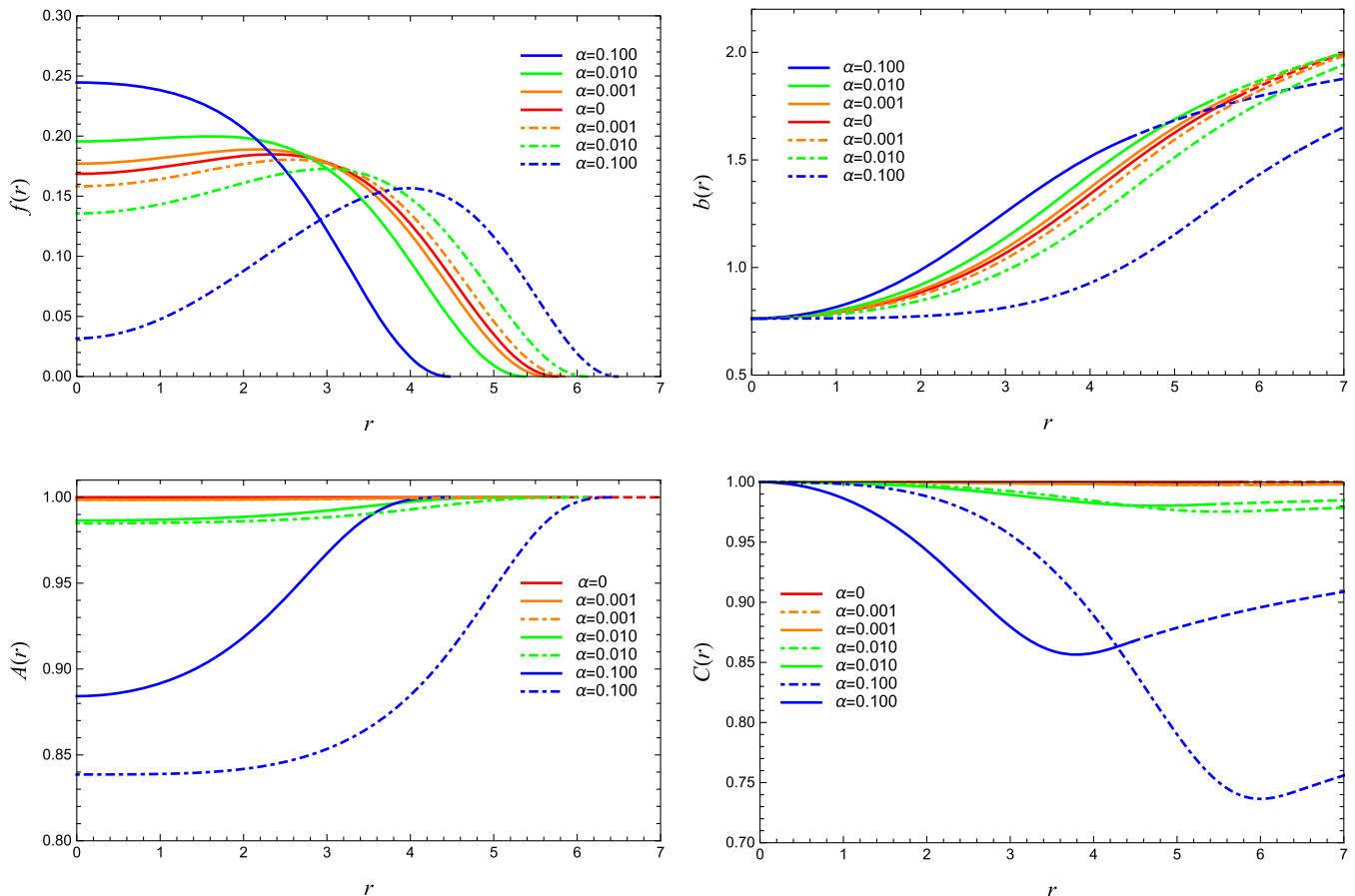


FIG. 6. The gauged gravitating  $Q$ -ball solution for the  $\mathbb{C}P^1$ . The parameter  $b_0$  is fixed as  $b_0 = 0.7627$ . Top left: the matter profile function  $f(r)$ . Top right: the gauge function  $b(r)$ . Bottom left: the metric function  $A(r)$ . Bottom right: the metric function  $C(r)$ . Solutions of the first branch are plotted with the bold line and those of the second branch are plotted with the dot-dashed line. Solutions of the vacuum equations are depicted with the dashed line. Distinct curves correspond with different values of the coupling constant  $\alpha$ .

shooting parameter, the second type of solutions look closer to the shell shape, but not to become exact because we do not impose the compact support in the interior. Therefore, the compactness condition (49) is essential for the scaling  $Q^{7/6}$ .

#### IV. THE GRAVITATING SOLUTIONS

The gravitating  $Q$ -balls and  $Q$ -shells are obtained by solving the differential Eqs. (22)–(25) with different  $n$ , We look at dependence of these solutions on the parameter  $b_0, \alpha$ . Here we present the numerical results for employing the value  $b_0$  of the vicinity of the bifurcation point, i.e., the point where the two branches merge. In Fig. 6, we plot the solution for the  $\mathbb{C}P^1$ . In similarity to the flat case, the profile function  $f(r)$  has nonzero value at the origin and reaches zero at the compacton radius. We also present the gauge function  $b(r)$  and the metric functions  $A(r), C(r)$ . A notable feature of the solution is emergence of the branches when varying the coupling constant  $\alpha$ . As  $\alpha$  increases, the first type of solution tends to shrink while the

second one grows. Figure 7 is the similar plot but for  $\mathbb{C}P^{11}$ . The relation between  $E^{-1/5}$  and  $Q^{-1/6}$  of the gravitation solutions is presented in Fig. 8.

We are able to consider the  $Q$ -shells with a massive body immersed in their center, which is referred as a harbor. In particular, there is a possibility of having this body as a Schwarzschild or a Reissner-Nordström type black hole [11,31,32,34]. We set the event horizon in the interior part of the shell and then solve the equations from the event horizon to the outer region. In order to find the harbor solutions, we follow a few steps. We assume the solution of the vacuum Einstein equation in the region between the event horizon and the inner boundary of the shell  $r \in [r_h, R_{in}]$  because matter function vanishes in this region. A similar approach is applied outside the shell  $r \in [R_{out}, \infty)$ . Next, we solve the equations in the region  $r \in (R_{in}, R_{out})$  and then smoothly connect the metric functions with such vacuum solutions at both boundaries. We present typical results in Fig. 9 for  $Q_H = 0.0001$ .

In Fig. 10, we plot  $E^{-1/5}-Q^{-1/6}$  relation for the harbor solutions of  $\mathbb{C}P^{11}$  with several values of  $b_0$ .

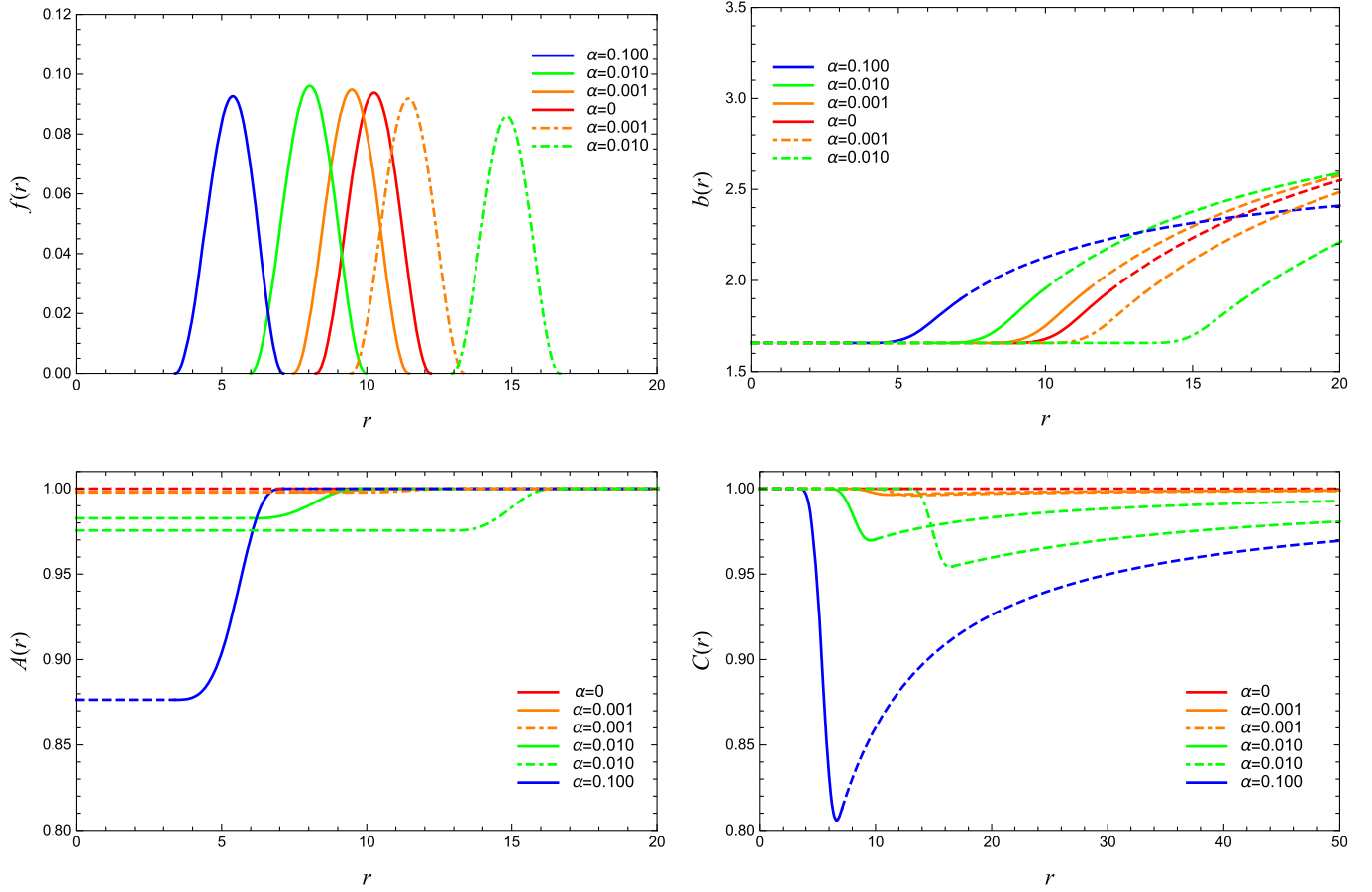


FIG. 7. The gauged gravitating  $Q$ -shell solution for the  $\mathbb{C}P^{11}$ . The parameter  $b_0$  is fixed as  $b_0 = 1.657$ . Top left: the matter profile function  $f(r)$ . Top right: the gauge function  $b(r)$ . Bottom left: the metric function  $A(r)$ . Bottom right: the metric function  $C(r)$ . Solutions of the first branch are plotted with the bold line and those of the second branch are plotted with the dot-dashed line. Solutions of the vacuum equations are depicted with the dashed line. Distinct curves correspond with different values of the coupling constant  $\alpha$ .

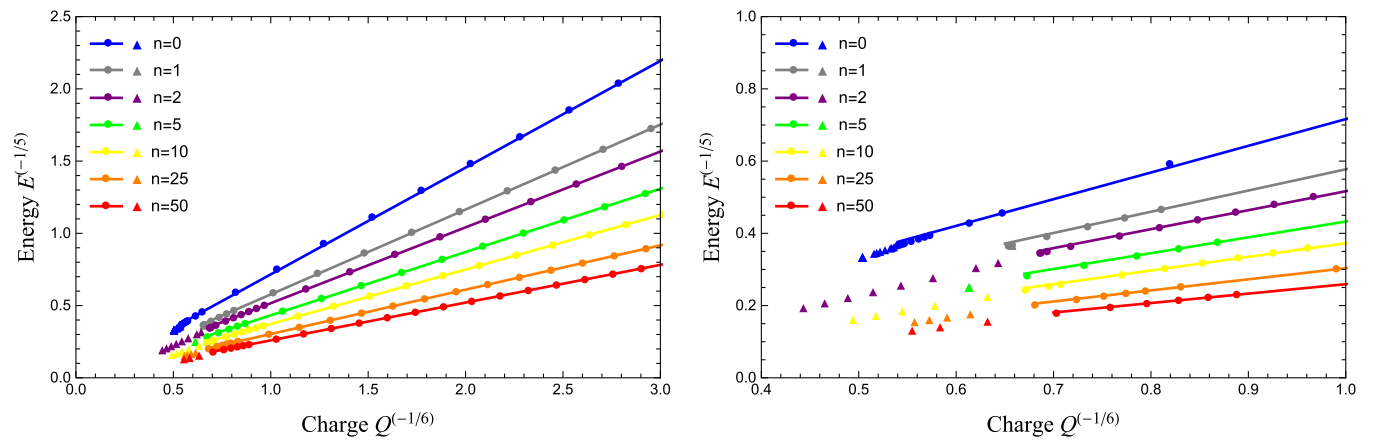


FIG. 8. Left: the relation between  $E^{-1/5}$  and  $Q^{-1/6}$  for several gauged solutions. Right: the same as the left one but the plot is enlarged in region of high  $Q, E$ . The parameter  $\alpha = 0.001$ . The dots correspond to solutions with  $\omega$  of the first branch. The triangles correspond to solutions of the second branch.

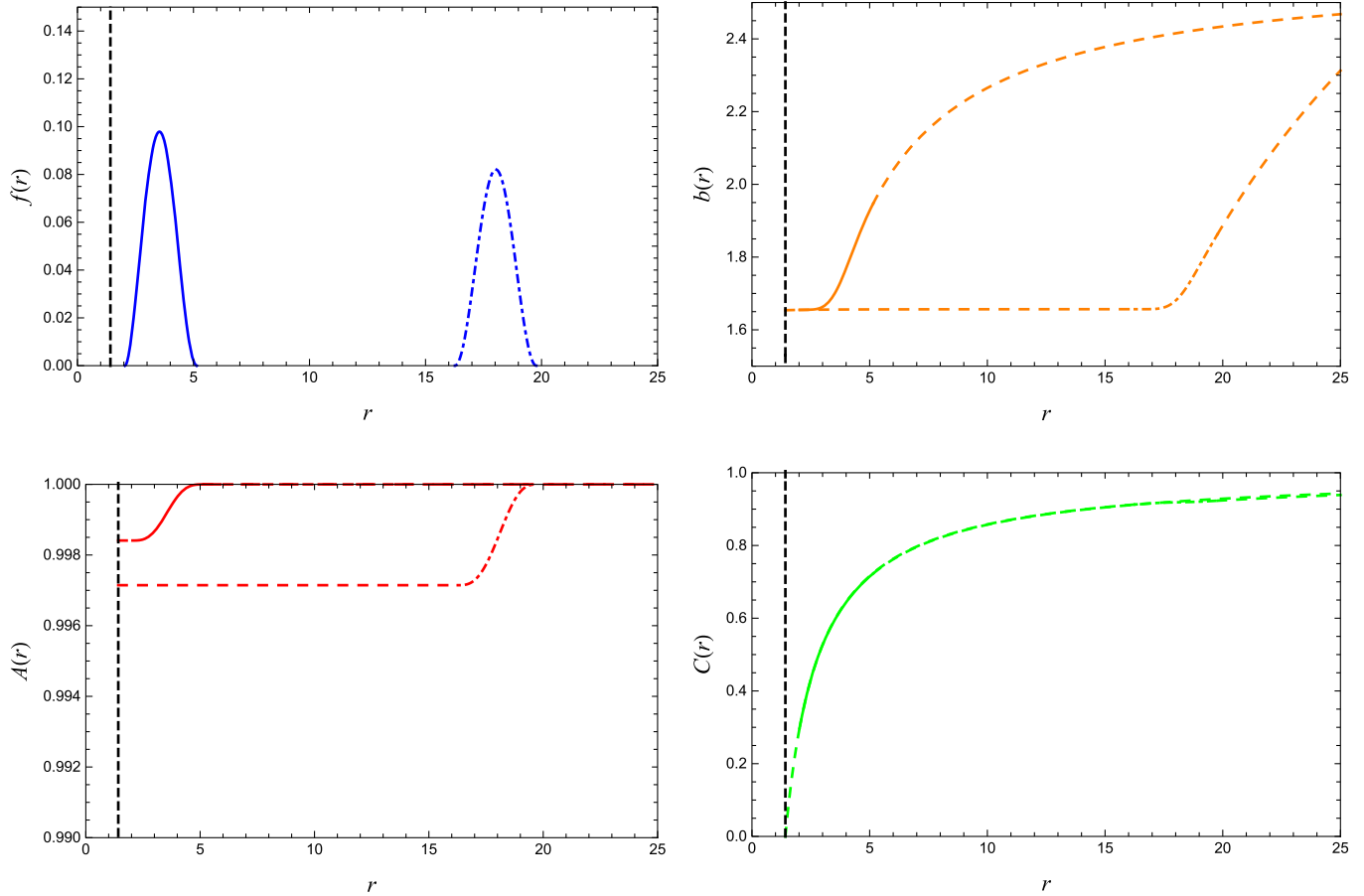


FIG. 9. The harbor solution for  $CP^{11}$  for a charged black hole. The parameters  $b_0 = 1.657$  and  $\alpha = 0.001$ . Top left: the matter profile function  $f(r)$ . Top right: the gauge function  $b(r)$ . Bottom left: the metric function  $A(r)$ . Bottom right: the metric function  $C(r)$ . Solutions of the first branch are plotted with the bold line and those of the second branch are plotted with the dot-dashed line. Solutions of the vacuum equations are depicted with the dotted line. The radius of the event horizon is chosen as  $r_H = 1.420$ .

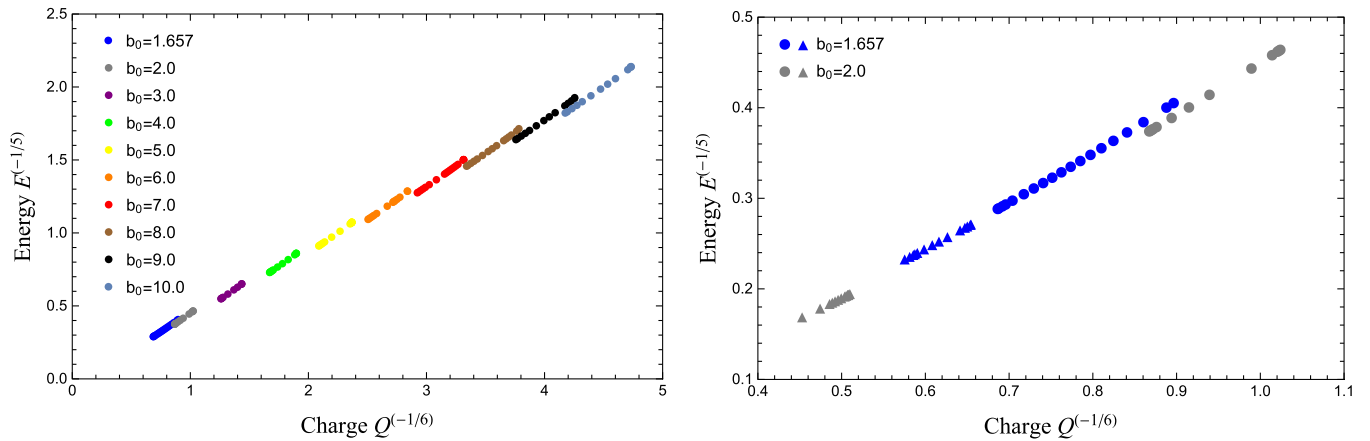


FIG. 10. Left: the relation between  $E^{-1/5}$  and  $Q^{-1/6}$  for harbor solutions of  $CP^{11}$ . The dots with the same color indicate the solutions which differ only by the value of a horizon radius  $r_H$ . The dots correspond to the first branch. Right: same as the left but the plots for  $b_0 = 1.657, 2.0$  are enlarged. The dots correspond to the first branch and the triangles to the second branch. The parameters  $\alpha = 0.001$ .

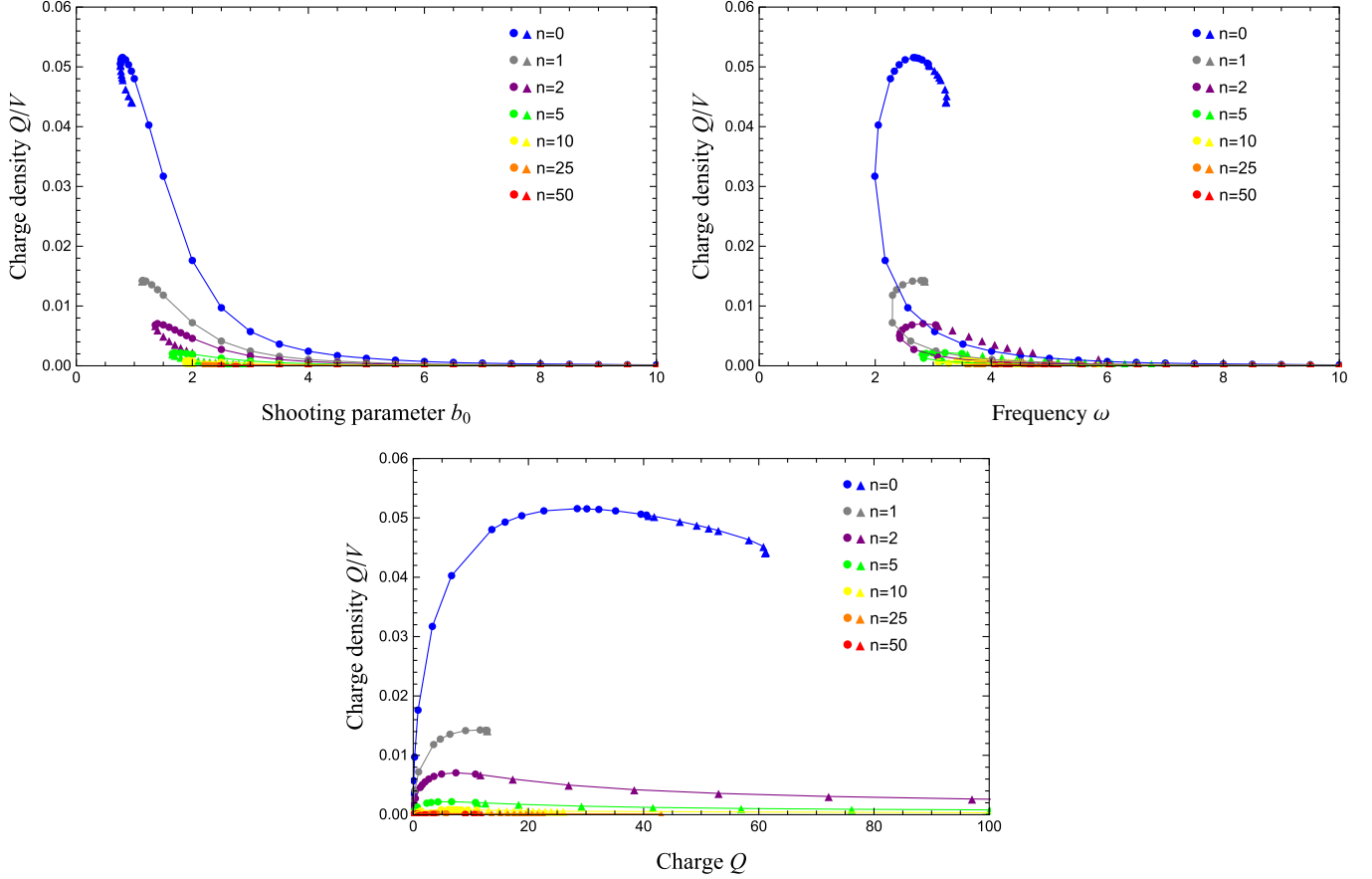


FIG. 11. The charge density: (the Noether charge  $Q$ )/(the volume of the  $Q$ -shell  $V$ ) for the several quantities of the model. Left top: for the shooting parameter  $b_0$ . Right top: for the frequency  $\omega$ . Bottom: the charge  $Q$ . The dots correspond to the first branch and the triangles to the second branch.

## V. FURTHER DISCUSSION

A salient feature of our  $U(1)$  gauged model is a deviation from the energy-charge scaling  $E \sim Q^{5/6}$  for large  $Q$ . Physically, we promptly guess that it is caused by the fact that the gauge field realizes the repulsive force between the constituents. The situation can be observed from the behavior of the solutions in Fig. 1. At the low density, the solution behaves as a lump. It begins to deform at the intermediate region and the solutions of the second type exhibit more delocalized, look like the shell structure, which apparently is effect of the repulsive electric force. In order to see the mechanism more qualitatively, we derive the charge density of our solutions. For simplicity, we employ the solutions of the flat space-time, but behavior of the gravitating solutions is quite similar. Thanks to the compactness of the solutions, we directly compute the volume of the  $Q$ -balls or  $Q$ -shells with the compacton radius  $r = R_{\text{in}}, R_{\text{out}}$ . In Fig. 11, we present the charge density as a function of the shooting parameters  $b_0$ , the frequency  $\omega$ , and the charge  $Q$ . For the parameter  $b_0$  or  $\omega$ , the density increases with the decrease in the parameters from the large values. Approaching the maximum of the

density, the solutions begin to deform and the density is relaxed. The solution moves on the second branch and the density turns to decreasing behavior. For the  $Q$ -shells, the energy scales as  $Q^{7/6}$ . For increasing the charge  $Q$ , the density also increases. The repulsive force by the electric interaction is effectively strong and then the solution deviates from  $Q^{5/6}$  behavior. After reaching the maximum, the solution relaxes for decreasing the density.

## VI. SUMMARY

In this paper, we have considered  $U(1)$  gauged  $CP^N$  nonlinear sigma model with a compact support in flat space-time and also coupled with gravity. We have obtained the compact  $Q$ -ball and  $Q$ -shell solutions in the standard shooting method. The resulting self-gravitating regular solutions form boson stars and boson shells. For the compact  $Q$ -shell solutions, we put the Schwarzschild-like black holes in the interior and the exterior of the shell that became the Reissner-Nordström space-time which may be a contradiction of the no hair conjecture.

In the  $U(1)$  gauged model, the energy-charge scaling deviates from the corresponding global model,

i.e.,  $E \sim Q^{5/6}$  for large  $Q$ . We discussed why the energy is enhanced for large  $Q$  region in terms of the simple analysis of the charge density. For large  $Q$ , the charge density grows and then the repulsive force that originates in the electric interaction dominates and then the solution tends to be unstable.

In [35–37], the authors have shown several beautiful phase diagrams concerning many bifurcation points and branches. Since our model shares some features with their model, we expect that we may observe the similar behaviors with our solutions. At present, we could see no explicit signal of the extra branches. Apparently, we need the numerical study with special care and it will be our subsequent study.

This paper is the first step for the construction of gravitating  $Q$ -balls (-shells) with non-Abelian symmetry  $SU(2) \otimes U(1)$ .  $Q$ -ball solutions with the symmetry  $SU(2) \otimes U(1)$  will certainly be possible to exist. It is interesting because two different types of Noether charges

corresponding to the symmetry have a crucial role in the stabilization of nontopological solitons. We shall report the results in our forthcoming paper.

## ACKNOWLEDGMENTS

The authors would like to thank Paweł Klimas for his careful reading of this paper and also for many useful advices and comments. We are also grateful for his kind hospitality of UFSC. We appreciate Yuki Amari, Atsushi Nakamura, and Kouichi Toda for valuable discussions. S. Y. is grateful to Betti Hartmann of useful discussions and also the kind hospitality of UPV/EHU where part of this work was done. S. Y. thanks the Yukawa Institute for Theoretical Physics at Kyoto University. Discussions during the YITP workshop YITP-W-19-10 on “Strings and Fields 2019” were useful to complete this work. N. S. is supported in part by JSPS KAKENHI Grants No. JP 16K01026 and No. B20K03278(1).

- 
- [1] R. Friedberg, T. D. Lee, and A. Sirlin, A class of scalar-field soliton solutions in three space dimensions, *Phys. Rev. D* **13**, 2739 (1976).
  - [2] S. R. Coleman,  $Q$  balls, *Nucl. Phys.* **B262**, 263 (1985); Erratum, *Nucl. Phys.* **B269**, 744 (1986).
  - [3] R. A. Leese,  $Q$  lumps and their interactions, *Nucl. Phys.* **B366**, 283 (1991).
  - [4] V. Loiko, I. Perapechka, and Y. Shnir,  $Q$ -balls without a potential, *Phys. Rev. D* **98**, 045018 (2018).
  - [5] R. Friedberg, T. D. Lee, and Y. Pang, Scalar soliton stars and black holes, *Phys. Rev. D* **35**, 3658 (1987).
  - [6] T. D. Lee, Soliton stars and the critical masses of black holes, *Phys. Rev. D* **35**, 3637 (1987).
  - [7] A. Kusenko, Solitons in the supersymmetric extensions of the standard model, *Phys. Lett. B* **405**, 108 (1997).
  - [8] A. Kusenko and M. E. Shaposhnikov, Supersymmetric  $Q$  balls as dark matter, *Phys. Lett. B* **418**, 46 (1998).
  - [9] A. Kusenko, V. Kuzmin, M. E. Shaposhnikov, and P. G. Tinyakov, Experimental Signatures of Supersymmetric Dark Matter  $Q$  Balls, *Phys. Rev. Lett.* **80**, 3185 (1998).
  - [10] P. Klimas and L. R. Livramento, Compact  $Q$ -balls and  $Q$ -shells in CPN type models, *Phys. Rev. D* **96**, 016001 (2017).
  - [11] P. Klimas, N. Sawado, and S. Yanai, Gravitating compact  $Q$ -ball and  $Q$ -shell solutions in the  $\mathbb{C}P^N$  nonlinear sigma model, *Phys. Rev. D* **99**, 045015 (2019).
  - [12] H. Arodz and J. Lis, Compact  $Q$ -balls in the complex sigum-Gordon model, *Phys. Rev. D* **77**, 107702 (2008).
  - [13] H. Arodz and J. Lis, Compact  $Q$ -balls and  $Q$ -shells in a scalar electrodynamics, *Phys. Rev. D* **79**, 045002 (2009).
  - [14] B. J. Schroers, Bogomolny solitons in a gauged  $O(3)$  sigma model, *Phys. Lett. B* **356**, 291 (1995).
  - [15] J. Gladikowski, B. M. A. G. Piette, and B. J. Schroers, Skyrme-Maxwell solitons in  $(2+1)$ -dimensions, *Phys. Rev. D* **53**, 844 (1996).
  - [16] F. Navarro-Lérida and D. H. Tchrakian, Vortices of  $SO(2)$  gauged skyrmions in  $2+1$  dimensions, *Phys. Rev. D* **99**, 045007 (2019).
  - [17] B. J. Schroers, Gauged sigma models and magnetic skyrmions, *SciPost Phys.* **7**, 030 (2019).
  - [18] D. H. Tchrakian and K. Arthur, Solitons in gauged sigma models: Two-dimensions, *Phys. Lett. B* **352**, 327 (1995).
  - [19] A. Y. Loginov, Topological solitons in a gauged  $CP(2)$  model, *Phys. Rev. D* **93**, 065009 (2016).
  - [20] K.-M. Lee, J. A. Stein-Schabes, R. Watkins, and L. M. Widrow, Gauged  $q$  balls, *Phys. Rev. D* **39**, 1665 (1989).
  - [21] K. N. Anagnostopoulos, M. Axenides, E. G. Floratos, and N. Tetradis, Large gauged  $Q$  balls, *Phys. Rev. D* **64**, 125006 (2001).
  - [22] T. S. Levi and M. Gleiser, Gauged fermionic  $Q$  balls, *Phys. Rev. D* **66**, 087701 (2002).
  - [23] I. E. Gulamov, E. Ya. Nugaev, and M. N. Smolyakov, Theory of  $U(1)$  gauged  $Q$ -balls revisited, *Phys. Rev. D* **89**, 085006 (2014).
  - [24] Y. Brihaye, V. Diemer, and B. Hartmann, Charged  $Q$ -balls and boson stars and dynamics of charged test particles, *Phys. Rev. D* **89**, 084048 (2014).
  - [25] T. Tamaki and N. Sakai, Large gauged  $Q$ -balls with regular potential, *Phys. Rev. D* **90**, 085022 (2014).
  - [26] I. E. Gulamov, E. Y. Nugaev, A. G. Panin, and M. N. Smolyakov, Some properties of  $U(1)$  gauged  $Q$ -balls, *Phys. Rev. D* **92**, 045011 (2015).
  - [27] V. Loiko and Y. Shnir,  $Q$ -balls in the  $U(1)$  gauged Friedberg-Lee-Sirlin model, *Phys. Lett. B* **797**, 134810 (2019).

- [28] A. Y. Loginov and V. V. Gauszstein, Radially excited  $U(1)$  gauged  $Q$ -balls, *Phys. Rev. D* **102**, 025010 (2020).
- [29] T. D. Lee and Y. Pang, Nontopological solitons, *Phys. Rep.* **221**, 251 (1992).
- [30] P. Jetzer, Boson stars, *Phys. Rep.* **220**, 163 (1992).
- [31] B. Kleihaus, J. Kunz, C. Lammerzahl, and M. List, Charged boson stars and black holes, *Phys. Lett. B* **675**, 102 (2009).
- [32] B. Kleihaus, J. Kunz, C. Lammerzahl, and M. List, Boson shells harbouring charged black holes, *Phys. Rev. D* **82**, 104050 (2010).
- [33] S. L. Liebling and C. Palenzuela, Dynamical boson stars, *Living Rev. Relativity* **15**, 6 (2012); Erratum, *Living Rev. Relativity* **20**, 5 (2017).
- [34] S. Yanai, Q-balls, -shells of a nonlinear sigma model with finite cosmological constants, *J. Phys. Conf. Ser.* **1194**, 012114 (2019).
- [35] S. Kumar, U. Kulshreshtha, and D. S. Kulshreshtha, Boson stars in a theory of complex scalar fields coupled to the  $U(1)$  gauge field and gravity, *Classical Quantum Gravity* **31**, 167001 (2014).
- [36] S. Kumar, U. Kulshreshtha, and D. S. Kulshreshtha, Boson stars in a theory of complex scalar field coupled to gravity, *Gen. Relativ. Gravit.* **47**, 76 (2015).
- [37] S. Kumar, U. Kulshreshtha, and D. S. Kulshreshtha, Charged compact boson stars and shells in the presence of a cosmological constant, *Phys. Rev. D* **94**, 125023 (2016).
- [38] B. Hartmann, B. Kleihaus, J. Kunz, and I. Schaffer, Compact boson stars, *Phys. Lett. B* **714**, 120 (2012).
- [39] B. Hartmann, B. Kleihaus, J. Kunz, and I. Schaffer, Compact (A)dS boson stars and shells, *Phys. Rev. D* **88**, 124033 (2013).
- [40] Y. Brihaye and B. Hartmann, Angularly excited and interacting boson stars and Q-balls, *Phys. Rev. D* **79**, 064013 (2009).
- [41] A. Bernal, J. Barranco, D. Alic, and C. Palenzuela, Multi-state boson stars, *Phys. Rev. D* **81**, 044031 (2010).
- [42] L. G. Collodel, B. Kleihaus, and J. Kunz, Excited boson stars, *Phys. Rev. D* **96**, 084066 (2017).
- [43] M. Alcubierre, J. Barranco, A. Bernal, J. C. Degollado, A. Diez-Tejedor, M. Megevand, D. Nunez, and O. Sarbach,  $\ell$ -Boson stars, *Classical Quantum Gravity* **35**, 19LT01 (2018).
- [44] M. Alcubierre, J. Barranco, A. Bernal, J. C. Degollado, A. Diez-Tejedor, M. Megevand, D. Nunez, and O. Sarbach, Dynamical evolutions of  $\ell$ -boson stars in spherical symmetry, *Classical Quantum Gravity* **36**, 215013 (2019).